IUST
Iran University of Science and Technology

Iranian Journal of Electrical and Electronic Engineering

Journal Homepage: ijeee.iust.ac.ir

Feasibility Analysis of Indoor 3D Localization System with UWB Using Least Squares Trilateration

Muhamad Naqib Mohd Shukri*, Syed Muhammad Mamduh Syed Zakaria**(C.A.), Ahmad Shakaff Ali Yeon*, Ammar Zakaria*, Latifah Munirah Kamarudin**

Abstract: Accurate 3D Localization is very important for a wide range of applications, such as indoor navigation, industrial robotics, and motion tracking. This research focuses on indoor 3D positioning systems using ultra-wideband (UWB) devices. Two localization experiments were conducted using the Least Squares Trilateration method. In the first experiment, anchors were at the same height, while in the second, they were at varying heights. The lowest percentage errors in the first experiment were 0% at the x-axis, 0.21% at the y-axis, and 19.75% at the z-axis. In the second experiment, the lowest percentage errors in the experiment were 1.98% at the x-axis, 0.68% at the y-axis, and 17.86% at the z-axis, demonstrating improved accuracy with varied anchor heights at the axis. This work shows the z-axis measurements are unreliable and noisy due to the limited intersection of signal waves of each anchor in a same height anchors setup.

Keywords: 3D Localization System, Ultra-Wideband, Trilateration.

1 Introduction

IN many applications, including monitoring, warehouse management systems, indoor navigation, and rescue operations, localization has grown in significance. These initiatives demonstrate how accurate location awareness is necessary to get the best outcomes. As a result, numerous methods and technologies targeted at precisely estimating target positions have undergone tremendous development [1]. Furthermore, there has been a significant convergence of technology with the sports and health industries in the domains of "smart sports" and "technological sports." Through this combination, high-tech solutions in the fitness and competitive sports domains are integrated and digitalized, leading to advancements in localization and positioning [2]. Because there is a high demand for a system that is ideal and not dependent on environmental conditions, indoor positioning has always been of great interest. Both accuracy and power efficiency are important performance requirements for these positioning techniques, with the latter depending on the particular use case for example, because vehicular access systems are usually battery-powered and must function for prolonged periods of time without frequent recharging, they require low power consumption on the tag side (e.g., car keys) [3]. Range, another name for distance measurement, is a key element in localization. Accurate time-of-flight (ToF) and time-difference-of-arrival (TDoA) measurements are difficult to obtain, though, for several reasons. Radio frequency signals must be timed with nanosecond to picosecond precision because they travel at the speed of light [13], [17]. Received-signal-strength (RSS), angle-of-arrival (AoA) [7], time-of-arrival (ToA) [8], [9], and time-difference-of-arrival (TDoA) [10], [11] are examples of common parameters for localization [15]. While the AoA method has limited application and requires an antenna array at every anchor, the RSS method is not sensitive to the

Iranian Journal of Electrical & Electronic Engineering, 2025.
Paper first received 26 Dec. 2024 and accepted 22 Feb. 2025.
* The author is with the Faculty of Electrical Engineering & Technology, Universiti Malaysia Perlis (UniMAP), Kampus Alam Pauh Putra 02600 Arau Perlis, Malaysia.
E-mails: muhamadnaqib@studentmail.unimap.edu.my, ahmadshakaff@unimap.edu.my, ammarzakaria@unimap.edu.my.
** The author is with the Faculty of Electronic Engineering & Technology, Universiti Malaysia Perlis (UniMAP), Kampus Alam Pauh Putra 02600 Arau Perlis, Malaysia.
E-mail: smmamduh@unimap.edu.my, latifahmunirah@unimap.edu.my

Corresponding Author: Syed Muhammad Mamduh Syed Zakaria.

channel environment. A sequence of time-stamp messages is exchanged between the anchor and the agent in the ToA and TDoA methods [16], [18]. By using time measurements, these time stamps enable the presentation of the ranging relationship between sensor nodes [20]. Nanosecond baseband narrow pulses are used in ultra-wideband (UWB) positioning technology, which functions as a carrier-free communication system [1]. Centimeter-level positioning accuracy is made possible by the high time resolution of UWB signals, which also greatly reduces system complexity and power consumption. UWB is distinguished from other positioning technologies by its low power consumption, low system complexity, high multipath resolution, and improved system security when compared to Bluetooth, Wi-Fi, Ultrasonic, RFID, and GNSS. The UWB technology widespread use in indoor and outdoor positioning applications can be attributed to these benefits [4]. An infrastructure-based indoor localization system typically consists of a target transceiver that is attached to the object that needs to be localized and a network of anchor transceivers that are fixed in place. This configuration, which is frequently used with UWB devices, shows how UWB technology can be applied practically to achieve accurate and effective localization [14]. The UWB radio is well-suited for indoor communications due to several features, including high immunity against wireless network interference and low susceptibility to multipath interference [5, 10]. Installing a UWB module (tag) on a person or object allows it to send ranging requests to fix UWB nodes at predetermined locations, or anchors, to achieve 3D positioning. Next, using anchor positions and tag distance measurements, the tag's position is determined [5]. Nevertheless, achieving high localization accuracy in diverse environmental scenarios remains a significant challenge. Although the accuracy of UWB-based localization systems could be improved, the Least Squares Trilateration method has not gotten enough attention in the literature up to this point. It is possible to achieve notable improvements in high-precision localization in complex environments by implementing and evaluating this strategy. Furthermore, it is imperative to investigate the effects on the z-axis value when the anchor height is at the same level and the anchors with various levels of height, as this may have a major bearing on the precision of 3D positioning. In this study, the localization experiment was conducted using UWB tags and UWB anchors device to collect data. The location of the tag will measure using time of flight (ToF) [19]. The experiment is conducted indoors. A localization engine is used to calculate the position of the UWB tag x, y and z, using intersection radius of each anchor that detects the tag like in Figure 1.

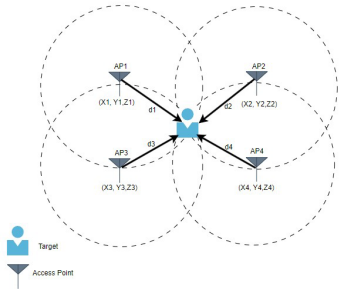

Fig.1. The Intersection radius of each anchor for tag detection [5]

2 Methodology

2.1 UWB Hardware

The experiment was conducted based on indoor mode in the research lab. The location of anchors was measured using a measuring tape. The tag was mounted on a tripod. The position of the tag varies for each experiment run, where each position is measured using a measuring tape to obtain its actual position. The number of tags used in each experiment is one tag. The tag and the anchor used in this work are shown in Figure 2. The one of the anchors (main anchor) is connected to a laptop via USB to enable data collection using a flutter-based software. The software was used to collect the time of flight (ToF) data of between each anchor with the tag.

(a) (b)

Fig.2. Figure (a) is the UWB Tag [8] meanwhile (b) is the UWB anchor [8] used to transmit and receive signal to detect tag radius.

The UWB Tag in Figure 2(a) can be used for person and object tracking using long range UWB technology that operates outside congested wi-fi bands signal. It utilizes UWB radio bands, operating in 3 to 7 GHz range, compliant with the IEEE 802.15.4a standard. The UWB tag is powered by 500mAH LiPo battery. The device has accuracy for indoor localization within 20 centimeters (cm). In general, for indoor environments, the maximum measuring range is 30 meters at 6.8Mbps. In an obstacle filled environment, the UWB radio signals can penetrate the obstacles, allowing for a true 3D tracking environment across an entire building. However, the experiments in this work were set up to specifically minimize the effects of signal degradation by obstacles

where the anchors and the tag were place inside a room with minimal human interference. The UWB radio also ensures a reliable connection, serving as a data backhaul for bi-directional secured communication, and it operates on globally permitted unoccupied frequencies outside the Wi-Fi spectrum. [8]

The UWB Anchor, system is infinitely scalable for large deployments and operates wirelessly, using globally allowed frequencies that are outside congested Wi-Fi band signals. The UWB Anchors incorporates a Qorvo UWB radio operating in the 3 to 7 GHz range, compliant with the IEEE 802.15.4a standard, it provides indoor and outdoor localization with an accuracy of less than 10 cm. The typical outdoor range for the UWB system extends up to 300 meters at 6.8 Mbps and have special electronics to enhance the sensitivity and selectivity of the radio transceiver. The UWB radio ensures a reliable connection, serving as a data backhaul for bi-directional communication, and operates on globally permitted 'unoccupied' frequencies outside the Wi-Fi spectrum. [8]

2.2 Experiment with Same Anchors Height

In this experiment, all anchors will be arranged in their designated positions while maintaining the same height. This setup will evaluate the performance of the localization engine using the Least Squares Trilateration method when the z-axis remains constant.The illustration arrangement of the anchor's location and tag's location is shown in Figure 3, for Experiment 1 tag position at (2000,1600,1650) Experiment 2 tag position at (3000,3300,525) and Experiment 3 tag position at (1500,5800,1000).

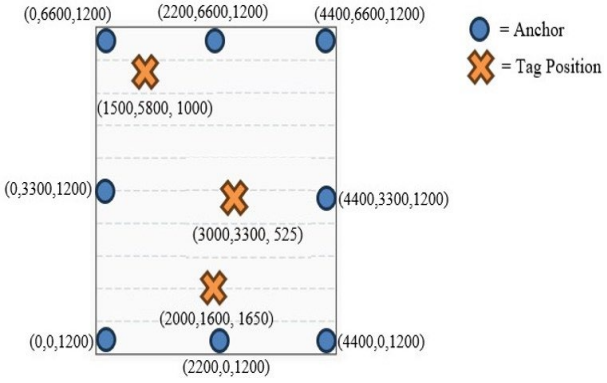

Fig.3. Project setup for fixed anchors position with same height for Experiment 1 is tag position at (2000,1600,1650) Experiment 2 tag position at (3000,3300,525) and Experiment 3 tag position at (1500, 5800,1000).

During each experiment, the tag transmitted its ToF measurement from each anchor every 5ms and received by the main anchor for data collection. It takes 80ms to complete 1 cycle of ToF measurement from all 8 anchors. Each experiment was conducted for 3 minutes and data that is not in the range of 0 to 6000 mm is discarded. The localization method uses the Least Squares Trilateration method as the localization process

2.3 Experiment with different Anchors Height

This experiment involves changing the arrangement of the anchors and tag to see the performance when the tag is far from anchor than before. Varying their heights of anchors to assess whether differing the z-axis leads to any improvement in the results. Figure 4 show the illustration arrangement of the anchor's location and tag's location for this experiment. There is three experiments with fixed position of anchors with variable tag positions. Experiment 1 tag position at (2200,4950,0) Experiment 2 tag position at (2200, 3300,1000) and Experiment 3 tag position at (4400,-500, 0).

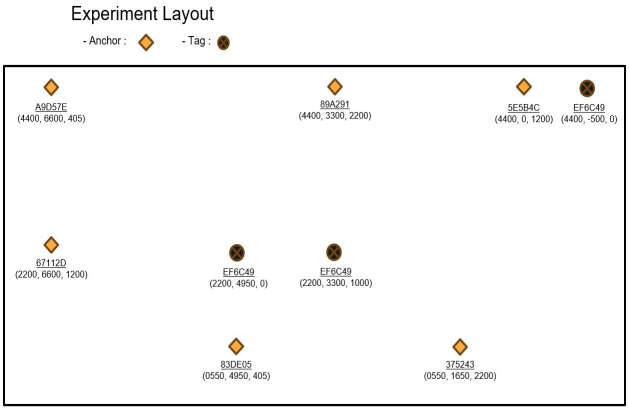

Fig.4. Project setup for fixed anchors position with different height, for Experiment 1 is tag position at (2200,4950,0) Experiment 2 tag position at (2200, 3300,1000) and Experiment 3 tag position at (4400,-500, 0).

Each experiment will repeat 3 times to ensure reliable and accurate results, experiments are repeated to identify anomalies, minimize the impact of random errors, and establish a stronger statistical foundation for drawing conclusions.

2.4 Least Squares Trilateration Method

Using localization engine, which is Least Square Trilateration method the information needed is the location of each anchor and the distance of each anchor with tag. From ToF value data from UWB devices, the Eq. (1) below is used to convert ToF to distance value. [9] D is distance, C is speed of light but in this work, C is replaced by manufacturer provided ToF to distance conversion coefficient value which is 4.617. Each experiment was conducted for 10 minutes torecord more data and data that is not in the range of -600mm to 6000 mm is discarded, with this range the negative data also can be collected.

$$D = ToF \times C$$

Find the unknown parameters x, y, z, and r using trilateration equation as shown in Eq. (2):

$$(x - \mathrm{a_x})^2 + (y - \mathrm{a_y})^2 + (z - \mathrm{a_z})^2 = \mathrm{d}^2$$

where:

x, y, z: The unknown coordinates of the tag being localized.

$\mathrm{a_x}$, $\mathrm{a_y}$, $\mathrm{a_z}$: known coordinates of an anchor.

d: The measured distance between the tag and the anchor.

Optimization Using Least Squares in Eq. (3):

$$F(x,y,z) = \sum_{i=1}^{n}\left((x - a_{x,i})(y - a_{y,i})(z - a_{z,i})\right)^2$$

where:

n: The number of anchors involved in the calculation.

$\mathrm{a_{x,i}}$, $\mathrm{a_{y,i}}$, $\mathrm{a_{z,i}}$: The coordinates of the *i*-th anchor.

d_i: The measured distance to the i-th anchor.

x, y, z: The unknown tag coordinates.

Calculate the error value Eq. (4):

$$\epsilon = ALE - Ac$$

where:

- *ALE* is average coordinate for x, y, or z that resulted from localization engine.

- *Ac* is actual coordinate for x, y, or z that measured that use measuring tape

Next, Eq. (5) the positioning error ($||\epsilon||$) to evaluate the localization performance [6]:

$$||\epsilon|| = \sqrt{\epsilon_x^2 + \epsilon_y^2 + \epsilon_z^2}$$

where, $\epsilon_x, \epsilon_y, \epsilon_z$ are represent error at average of x, y, and z.

Calculate the error value using percentage error formula in Eq. (6):

$$pe = \left|\frac{Avc - Ac}{Ac} \times 100\right|$$

where:

- *pe* is percentage error that always positive value

- *Avc* is average measure coordinate for x, y, or z

- *Ac* is actual coordinate for x, y, or z

3 Results

3.1 Result Experiment with Same Anchors Height

This section will show the result data from the location engine that used Least Square Trilateration that calculates the value of x, y, and z coordinates for 3 static localizations for 3 minutes. Figure 5 and Figure 6 show the result from experiment 1, Figure 5 is 2D for x vs y axis and Figure 6 in 3D for axis x, y, z. The actual position is (2200, 1600, 1650) mm plotted in Figures in X symbol. Table 1 shows the actual value to compare with average coordinate at Table 2. From Figures 5 and 6, it can be observed that the measured values are spread lower than the actual coordinates across the x, y, and z axes. The average coordinates in Table 2 provide evidence supporting this observation, showing that the plotted values are consistently lower than the actual coordinates in Table 1.

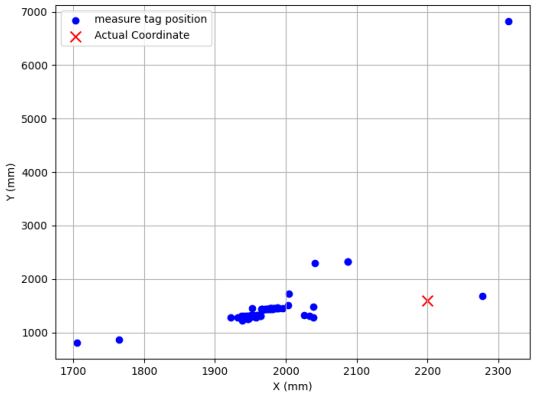

Fig.5. 2D plot result experiment 1 with actual value at (2200, 1600) mm.

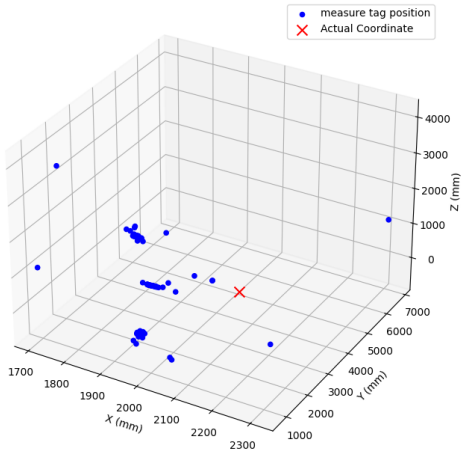

Fig.6. 3D plot result experiment 1 with actual value at (2200, 1600,1650) mm.

Table 1. Actual coordinate experiment 1

Actual Coordinate (mm)		
x	**y**	**z**
2200.00	1600.00	1650.00

Table 2. Average coordinate experiment 1

Average Coordinate (mm)		
x	**y**	**z**
1971.69	1455.53	1266.60

In Figure 7 and Figure 8 shows the result from experiment 2, Figure 7 is 2D for x and y axis and Figure 8 in 3D resulted in x, y, z axis. The actual position is (3000, 3300, 525) mm plotted in Figures in X symbol. Table 3 shows the actual coordinate value and the average coordinate in Table 4. From the Figure 7 and Figure 8 the measure plot result is spread closer to the actual value, in Table 4 show the average coordinate is close to the actual coordinate as shown in Table 3, except for z axis with over 300mm different.

In Figure 9 and Figure 10 shows the result from experiment 3, Figure 9 is 2D for x and y axis and Figure 10 in 3D resulted in x, y, z axis. The actual position is (1500, 5800, 1000) mm plotted in Figures in X symbol. Table 5 shows the average coordinate value and the actual value in Table 6. Figure 9 show measure plot is closer to the actual plot with a small difference around 10 mm for axis x and y. Figure 10 shows all the measure plot is plotted higher than actual plot at the z axis with difference around 190 mm. Table 6 show the average for x and y axis have only small differences than actual coordinate in Table 5, meanwhile average for z axis have high different with 197.49mm higher than actual value.

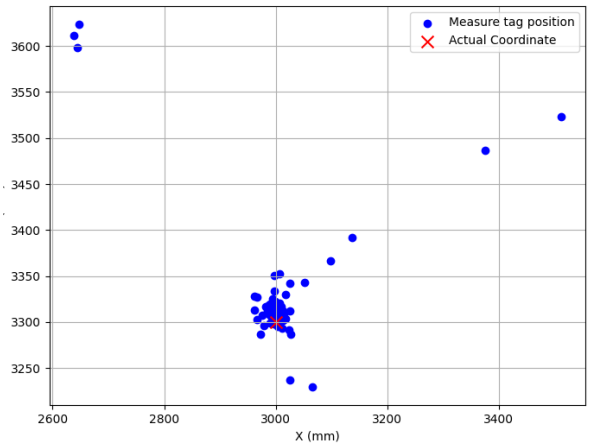

Fig.7. 2D plot result experiment 2 with actual value at (3000, 3300) mm.

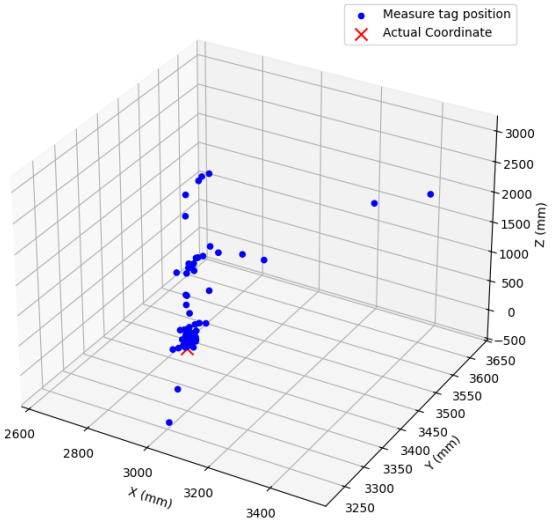

Fig.8. 3D plot result experiment 2 with actual value at (3000, 3300,525) mm.

Table 3. Actual coordinate experiment 2

Actual Coordinate (mm)		
x	**y**	**z**
3000.00	3300.00	525.00

Table 4. Average coordinate experiment 2

Average Coordinate (mm)		
x	**y**	**z**
3000.00	3321.54	870.54

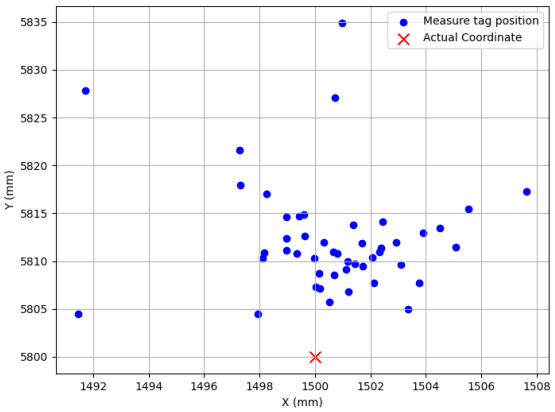

Fig.9. 2D plot result experiment 3 with actual value at (1500, 5800) mm.

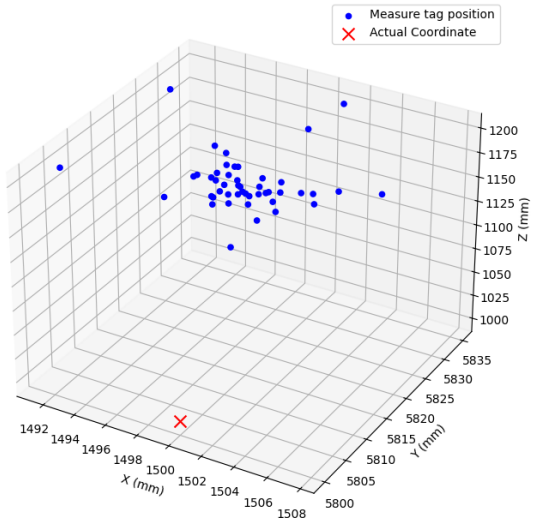

Fig.10. 3D plot result experiment 3 with actual value at (1500, 5800,1000) mm.

Table 5. Actual coordinate experiment 3

Actual Coordinate (mm)		
x	**y**	**z**
1500.00	5800.00	1000.00

Table 6. Average coordinate experiment 3

Average Coordinate (mm)		
x	**y**	**z**
1500.66	5812.33	1197.49

The percentage error for each coordinate (x, y, and z) was calculated to determine which axis had the highest or lowest error in each experiment, providing a basis for discussing the results. Table 7 shows that in experiment 1, the highest percentage error occurs when the actual coordinates are at (2200, 1600, 1650) mm. This may be due to the tag's position being close to only one anchor, while the other anchor is farther away, introducing noise during signal transmission. In Experiment 2, with actual coordinates at (3000, 3300, 525) mm, the percentage error is acceptable because the tag is positioned roughly in the middle of all the anchors. However, the z-axis has a higher percentage error, possibly because the tag's height is lower than the anchors, which are positioned at a height of 1200 mm. Experiment 3 which coordinate at (1500, 5800, 1000) mm shows the lowest percentage error for the x, y, and z coordinates compared to the other experiments. This can be attributed to the tag being near multiple anchors and the anchors' height of 1000 mm being relatively close to the tag height of 1200 mm.

Table 7. Percentage error each axis x, y, and z

Experiment	Percentage Error (%)		
	x	**y**	**z**
1	10.38	9.03	23.24
2	0	0.65	65.82
3	0.04	0.21	19.75

Positioning error is ranging based results typically refers to the difference between the estimated position of a tag and its actual location. The results from Table 8 proof that the lowest positioning error is at experiment 3 when the difference between average coordinate and actual coordinate at x, y, z is smallest.

Table 8. Positioning error every experiment

Experiment	Positioning Error /‖ϵ‖ (mm)
1	1139.10
2	367.25
3	198.01

3.2 Result Experiment with different Anchors Height

This section presents the results of the localization experiment conducted with anchors arranged at varying heights and a new configuration of anchors and the tag, where the distance between the tag and the anchors is greater than in previous setups. The experiment was repeated three times, as shown Run in the tables and each run lasted 10 minutes.

Table 9 presents the three Runs of results for Experiment 1, where the actual coordinates are (2200, 4950, 0) mm. The average measured coordinates across all versions are very close to the actual values, demonstrating the reliability of the data. For the x and y axes, the measured values are near the true coordinates, but the z-axis shows a significantly high negative value. Figure 11 illustrates the data spread around the actual coordinates on the x and y axes, while Figure 12 shows the z-axis data spreading further into negative coordinates for Experiment 1.

Table 9. The average coordinate Experiment 1 with actual value (2200, 4950, 0) mm.

	Average Coordinate (mm)		
Run	**x**	**y**	**z**
1	2123.01	4916.32	-171.66
2	2110.06	4913.73	-181.23
3	2113.24	4919.18	-182.95

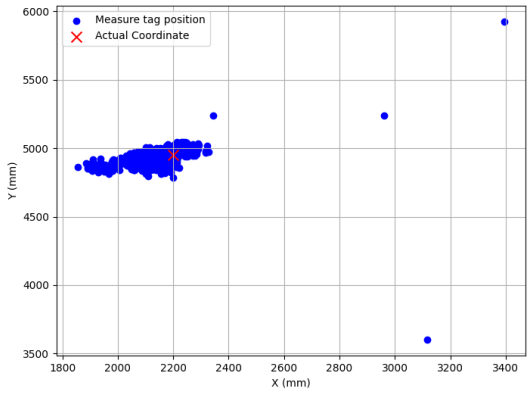

Fig.11. 2D plot result experiment 1 with actual value at (2200, 4950) mm.

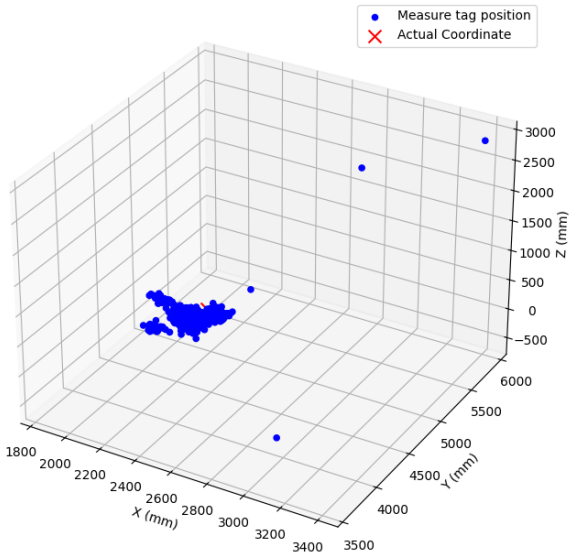

Fig.12. 3D plot result experiment 3 with actual value at (2200, 4950,0) mm.

Table 10 presents the three Runs of the average measured coordinates for Experiment 2, where the actual coordinates are (2200, 3300, 1000) mm. All versions are consistent with each other, making the data suitable for analysis. Table 7 show the x and y values are close to the actual coordinates, while the z-axis shows an average value approximately 270 mm lower than the actual coordinate. Figure 13 illustrates that the measured coordinates for Experiment 2 are close to the actual coordinates, with the data for the x and y axes slightly lower than the actual values. Similarly, the z-axis data, shown in Figure 14, also trends lower than the actual coordinate.

Table 10. The average coordinate Experiment 1 with actual value (2200, 3300, 1000) mm.

	Average Coordinate (mm)		
Run	**x**	**y**	**z**
1	2112.38	3179.07	724.88
2	2112.48	3181.24	727.45
3	2118.79	3182.97	730.5

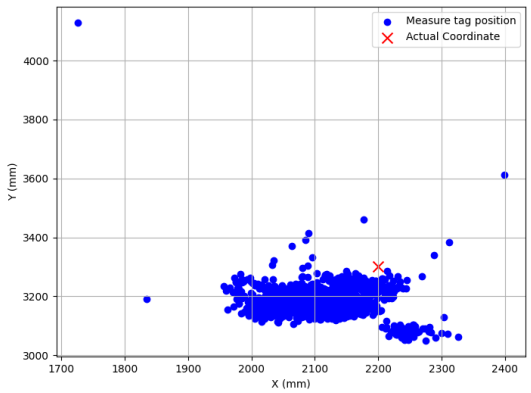

Fig.13. 2D plot result experiment 1 with actual value at (2200, 3300) mm.

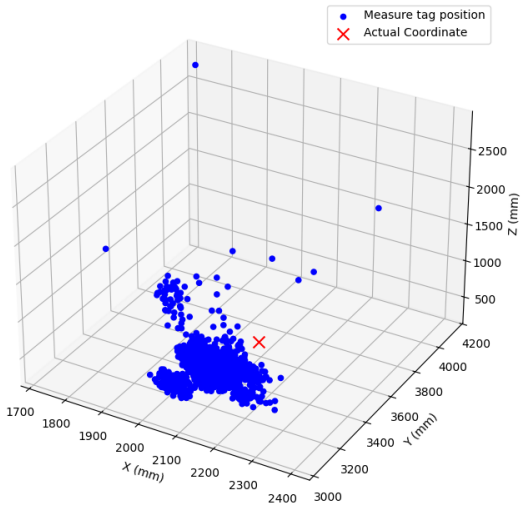

Fig.14. 3D plot result experiment 3 with actual value at (2200, 3300,1000) mm.

Table 11 presents the average measured coordinates for Experiment 3, where the actual coordinates are (4400, -500, 0) mm. All Runs in Table 11 are consistent and close to each other, indicating that the data is reliable for analysis. The average coordinates for the x and y axes are close to the actual values, while the z-axis is significantly lower, with a difference of approximately -200 mm. Figure 15 shows that the measured coordinates for the x and y axes are spread closer to the actual values. However, Figure 16 reveals that the measured values for the z-axis are spread negatively, deviating from the actual value of 0 mm in Experiment 3.

Table 12 shows the percentage error calculated from the average Run results of each experiment for the x, y, and z coordinates. The percentage error for the x and y axes is highly acceptable due to the low error values.

Table 11. The average coordinate Experiment 1 with actual value (4400, -500, 0) mm.

	Average Coordinate (mm)		
Run	**x**	**y**	**z**
1	4327.4	-547.04	-198.4
2	4305.73	-545.7	-255.1
3	4305.43	-547.09	-228.92

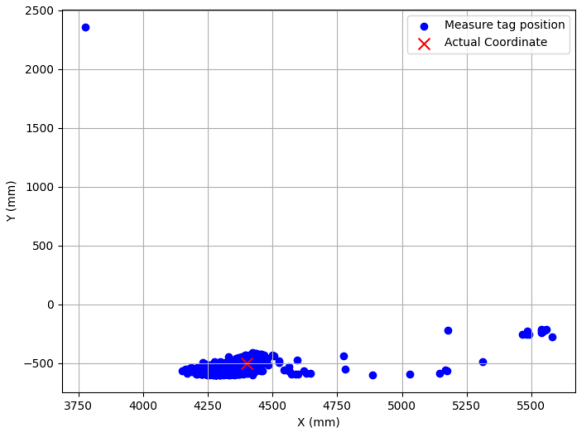

Fig.15. 2D plot result experiment 1 with actual value at (4400, -500) mm.

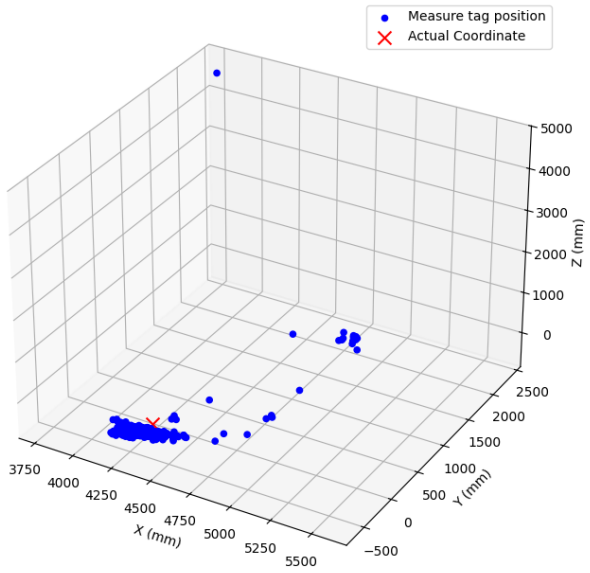

Fig.16. 3D plot result experiment 3 with actual value at (4400, -500, 0) mm.

Table 12. Percentage error each axis x, y, and z

Experiment	Percentage Error (%)		
	x	y	z
1	3.84	0.68	17.86
2	3.88	3.6	27.24
3	1.98	9.32	22.75

Furthermore, given the 10-minute experiment duration, some noise over time is expected. Data for z-axis coordinate, the percentage error is also acceptable as the error values are small and measured in millimeters. However, the higher percentage error on the z-axis can be attributed to specific conditions. In experiments 1 and 3, the tag position on the z-axis is 0 mm, while the lowest anchor height is 405 mm, making it difficult for the anchor signals to accurately optimize the tag's real value. Similarly, in experiment 2, the tag position on the z-axis is 1000 mm, while the nearest anchors are positioned at 405 mm and 2000 mm, which also complicates signal optimization for determining the tag's true value.

Positioning error is ranging based results typically refers to the difference between the estimated position of a tag and its actual location. The results from Table 13 proof that the lowest positioning error is at experiment 1 when the difference between average coordinate and actual coordinate at x, y, z is smallest.

Table 13. Positioning error every experiment

Experiment	Positioning Error /‖ϵ‖ (mm)
1	200.45
2	309.25
3	248.01

4 Conclusions

The experiments demonstrate the critical role of anchor configurations in determining the accuracy of range-based positioning systems. The experiments which is conducted with anchors at the same height, the percentage error was influenced by the relative positions of the tag and anchors. Experiment 1 exhibited the highest error, attributed to the tag being close to only one anchor, causing uneven signal distribution. Experiment 2 showed acceptable errors, with the tag positioned near the center of the anchors, though the z-axis error was higher due to the tag's lower height relative to the anchors. Experiment 3 achieved the lowest errors across all axes, benefiting from a closer alignment of tag and anchor heights. In experiments with varied anchor heights, the x and y axes consistently produced low errors, while the z-axis errors were higher due to challenges in optimizing signals when the tag height significantly differed from the anchors. To improve accuracy, future studies should incorporate anchors at diverse heights and setup the height of anchors in closer range of tag's height. Next, apply noise filtering techniques, and explore alternative localization methods. These findings underscore the importance of strategic anchor placement and advanced signal processing in achieving reliable and precise localization results.

Acknowledgements

The authors would like to acknowledge the support from the Fundamental Research Grant Scheme (FRGS) under the grant number FRGS/1/2020/TK0/UNIMAP /02/14 and FRGS-EC/1/2024/TK07/UNIMAP/02/29 and Industrial Matching Programme (IMaP) under the grant number IMaP/1/2024/TK07/UNIMAP//3.

References

[1] H. Pan, X. Qi, M. Liu, and L. Liu, "Indoor scenario-based UWB anchor placement optimization method for indoor localization," Expert Systems With Applications, vol. 205, p. 117723, Nov. 2022, doi: 10.1016/j.eswa.2022.117723.

[2] Y. Han, X. Zhang, Z. Lai, and Y. Geng, "TOF-Based Fast Self-Positioning Algorithm for UWB Mobile Base Stations," Sensors, vol. 21, no. 19, p. 6359, Sep. 2021, doi: 10.3390/s21196359.

[3] R. Mazraani, M. Saez, L. Govoni, and D. Knobloch, "Experimental results of a combined TDOA/TOF technique for UWB based localization systems," May 2017, doi: 10.1109/iccw.2017.7962796.

[4] C. Li et al., "CRLB-based Positioning Performance of Indoor Hybrid AoA/RSS/ToF Localization," Sep. 2019, doi: 10.1109/ipin.2019.8911771.

[5] Geok, T. K., Aung, K. Z., Aung, M. S., Soe, M. T., Abdaziz, A., Liew, C. P., Hossain, F., Tso, C. P. and Yong, W. H., Review of Indoor Positioning: Radio Wave Technology, Applied Sciences, vol. 11, no. 1, p. 279, from https://doi.org/10.3390/app11010279, December 30, 2020. DOI: 10.3390/app11010279

[6] Ferrigno, L., Miele, G., Milano, F., Pingerna, V., Cerro, G. and Laracca, M., A UWB-Based Localization System: Analysis of the Effect of Anchor Positions and Robustness Enhancement in Indoor Environments, from https://doi.org/10.1109/i2mtc50364.2021.9459845, May 17, 2021. DOI: 10.1109/i2mtc50364.2021.9459845

[7] Madfolio, Least-Squares-Trilateration/README.Md at Master · Madfolio/Least-Squares-Trilateration, GitHub, n.d.

[8] Airtls, AIRTLS Sport | Precise Real-Time Locating Combined with Innovative Analyses, n.d.

[9] Yasukawa, Y., Higashi, Y., Masuda, A. and Miura, N., Automatic Anchor Caliburation for UWB-Based Indoor Positioning Systems, from https://doi.org/10.1109/tencon50793.2020.9293741, November 16, 2020. DOI: 10.1109/tencon50793.2020.9293741

[10] Alrajeh, N. A., Bashir, M. and Shams, B., Localization Techniques in Wireless Sensor Networks, International Journal of Distributed Sensor Networks, vol. 9, no. 6, p. 304628, from https://doi.org/10.1155/2013/304628, June 1, 2013. DOI: 10.1155/2013/304628

[11] Win, M. Z., Buehrer, R. M., Chrisikos, G., Conti, A. and Poor, H. V., Foundations and Trends in Localization Technologies — Part I [Scanning the Issue], Proceedings of the IEEE, vol. 106, no. 6, pp. 1019–21, from https://doi.org/10.1109/jproc.2018.2837342, June 1, 2018. DOI: 10.1109/jproc.2018.2837342

[12] Chen, H. and Dhekne, A., Spoofing Evident and Spoofing Deterrent Localization Using Ultra-Wideband (UWB) Active-Passive Ranging, IEEE Journal of Indoor and Seamless Positioning and Navigation, vol. 2, pp. 12–24, from https://doi.org/10.1109/jispin.2023.3343336, January 1, 2024. DOI: 10.1109/jispin.2023.3343336

[13] Wang, T., Xiong, H., Ding, H. and Zheng, L., Automatic Setup Method for Anchor Coordinate in Asynchronous Localization System, 2020 5th International Conference on Computer and Communication Systems (ICCCS), from https://doi.org/10.1109/icccs49078.2020.9118486, May 1, 2020. DOI: 10.1109/icccs49078.2020.9118486

[14] Wang, Y. and Ho, K. C., Unified Near-Field and Far-Field Localization for AOA and Hybrid AOA-TDOA Positionings, IEEE Transactions on Wireless Communications, vol. 17, no. 2, pp. 1242–54, from https://doi.org/10.1109/twc.2017.2777457, February 1, 2018. DOI: 10.1109/twc.2017.2777457

[15] Le, T.-K. and Ono, N., Closed-Form and Near Closed-Form Solutions for TOA-Based Joint Source and Sensor Localization, IEEE Transactions on Signal Processing, vol. 64, no. 18, pp. 4751–66, from https://doi.org/10.1109/tsp.2016.2569465, September 15, 2016. DOI: 10.1109/tsp.2016.2569465

[16] Meyer, F., Tesei, A. and Win, M. Z., Localization of Multiple Sources Using Time-Difference of Arrival Measurements, from https://doi.org/10.1109/icassp.2017.7952737, March 1, 2017. DOI: 10.1109/icassp.2017.7952737

[17] Xiong, H., Chen, Z., An, W. and Yang, B., Robust TDOA Localization Algorithm for Asynchronous Wireless Sensor Networks, International Journal of Distributed Sensor Networks, vol. 11, no. 5, p. 598747, from https://doi.org/10.1155/2015/598747, May 1, 2015. DOI: 10.1155/2015/598747

[18] Mazraani, R., Saez, M., Govoni, L. and Knobloch, D., Experimental Results of a Combined TDOA/TOF Technique for UWB Based Localization Systems, from https://doi.org/10.1109/iccw.2017.7962796, May 1, 2017. DOI: 10.1109/iccw.2017.7962796

[19] Park, J. and Ko, Y.-B., PedLoc: UWB-Based Pedestrian Localization for Autonomous Vehicles, Internet of Things, vol. 26, p. 101194, from https://doi.org/10.1016/j.iot.2024.101194, July 1, 2024. DOI: 10.1016/j.iot.2024.101194

[20] Henry, J., Ranging and Positioning with UWB, in IntechOpen eBooks, from https://doi.org/10.5772/intechopen.109750, 2023.

Biographies

Muhamad Naqib Mohd Shukri received diploma in Mechatronics Engineering, University Malaysia Perlis, in 2019 and Bachelors in Mechatronics Engineering with Honours, University Malaysia Perlis in 2023. He is a Researcher and a Master of Science (M.Sc) student with Centre of Excellence for Advanced Sensor Technology (CEASTech), University Malaysia Perlis.

Associate Professor Dr. Syed Muhammad Mamduh Syed Zakaria received Bachelor Degree of Engineering (B. Eng), Mechatronic Engineering, University of Canterbury New Zealand in 2010 and Doctor of Philosophy (Ph.D) in Mechatronic Engineering from Universiti Malaysia Perlis in 2017. He is currently a Senior Lecturer Faculty of Electronic Engineering & Technology (FKTEN), Universiti Malaysia Perlis.

Dr.Ahmad Shakaff Bin Ali Yeon received Bachelor Degree of Engineering (B.Eng) Electrical and Electronic Engineering, Nagoya University, Japan in 2014 and Master of Science (M.Sc), Computer Engineering Universiti Malaysia Perlis, in 2017 and also Doctor of Philosophy (Ph.D), Mechatronic Engineering Universiti Malaysia Perlis, in 2023. He is currently a Senior Lecturer Faculty of Electrical Engineering & Technology (FTKE), Universiti Malaysia Perlis.

Associate Professor Dr. Ammar Zakaria received a First-Class Honours bachelor's degree in Electrical and Electronic Engineering from Portsmouth University, U.K., and a Ph.D. in Mechatronic Engineering from Universiti Malaysia Perlis (UniMAP). He is currently an associate researcher at the Centre of Excellence for Advanced Sensor Technology (CEASTech). His research interests focus on sensor technology, artificial intelligence, Industry 4.0 (IR 4.0), and the Internet of Things (IoT).

Associate Professor Dr. Latifah Munirah Kamarudin earned a First-Class Honours degree in Computer Science and Media Engineering from the University of Yamanashi, Japan, and a Doctor of Philosophy in Computer Network and Comm. Engineering from Universiti Malaysia Perlis. Recognized as one of Malaysia's Top Research Scientists, specializes in wireless sensing and artificial intelligence. As the Head of the Center of Excellence for Advanced Sensor Technology, she spearheads innovations in non-contact methods for continuous vital sign monitoring using AI, with a particular emphasis on addressing the needs of ageing societies. She also serves as a Visiting Professor at the University of Yamanashi, where she co-supervises students and engages in collaborative research.